Optomechanical trapping and cooling of partially reflective mirrors

M. Bhattacharya, H. Uys, and P. Meystre
B2 Institute, Department of Physics and College of Optical Sciences, The University of Arizona, Tucson, Arizona 85721, USA
(Received 29 August 2007; published 7 March 2008)

We consider the radiative trapping and cooling of a partially reflecting mirror suspended inside an optical cavity, generalizing the case of a perfectly reflecting mirror previously considered [M. Bhattacharya and P. Meystre, Phys. Rev. Lett. **99**, 073601 (2007)]. This configuration was recently used in an experiment to cool a nanometers-thick dielectric membrane [J. D. Thompson *et al.*, e-print arXiv:0707.1724v2]. The self-consistent cavity field modes of this system depend strongly on the position of the middle mirror, leading to important qualitative differences in the radiation pressure effects: in one case, the situation is similar to that of a perfectly reflecting middle mirror, with only minor quantitative modifications. In addition, we also identify a range of mirror positions for which the radiation-mirror-coupling becomes purely dispersive and the back-action effects that usually lead to cooling are absent, although the mirror can still be optically trapped. The existence of these two regimes leads us to propose a bichromatic scheme that optimizes the cooling and trapping of partially reflective mirrors.

DOI: 10.1103/PhysRevA.77.033819 PACS number(s): 42.50.Pq, 04.80.Nn, 42.65.Sf, 85.85.+j

I. INTRODUCTION

The optomechanical cooling and trapping of mirrors has recently become the subject of an intense research effort as it offers a viable means of extending quantum mechanics to macroscopic objects [1–5]. The typical experimental arrangement consists of a linear two-mirror optical cavity (2MC) driven by laser radiation close to a cavity resonance [Fig. 1(a)]. One of the mirrors in the cavity is small and is mounted on a cantilever, so as to be movable, and the goal is to cool its vibrational state of motion to a point as close to its quantum mechanical ground state as possible. The cooling proceeds with the use of two laser beams, the first one detuned to the blue of a cavity resonance and providing an optical trap for the movable mirror, with a frequency $\omega_{\rm eff}$ larger than the intrinsic cantilever frequency ω_M and the second one detuned to the red of the cavity, so as to (almost) independently increase the damping constant of the oscillating mirror from its field-free value D_M to $D_{\rm eff}$ [5].

From the quantum mechanical point of view, the combined effect of the laser fields on the moving mirror is twofold: they create a harmonic trap with large energy level spacing $\hbar\omega_{\rm eff}$, and cool the mirror from its initial equilibrium temperature T_e to a lower value

$$T_{\rm eff} = \left(\frac{D_M}{D_{\rm eff}}\right) T_e \tag{1}$$

as shown explicitly in Appendix A. The trapping and cooling effects thus lower the number of quanta of vibrational excitation of the oscillating mirror to

$$n_M = \frac{k_B T_{\rm eff}}{\hbar\omega_{\rm eff}} = \frac{k_B T_e}{\hbar\omega_{\rm eff}}\left(\frac{D_M}{D_{\rm eff}}\right), \tag{2}$$

where k_B is Boltzmann's constant. Current experimental efforts are intensely focused on achieving $n_M < 1$, i.e., at placing the mirror in its quantum mechanical ground state. We note at the outset that the expression for n_M given in Ref. [6] includes an additional factor $(\Omega_M/\Omega_{\rm eff})^3$ as compared to Eq. (2). That additional term results from expressing $T_{\rm eff}$ in terms of the "bare" oscillation frequency of the moving mirror rather than its effective frequency. When misinterpreted and applied to $\omega_{\rm eff}$ rather than ω_M it therefore underestimates the degree of excitation of the mirror. While this does not bring any qualitative change to the conclusions of the earlier work, the correct formula is Eq. (2). This same point has recently also been realized by other authors [8,9].

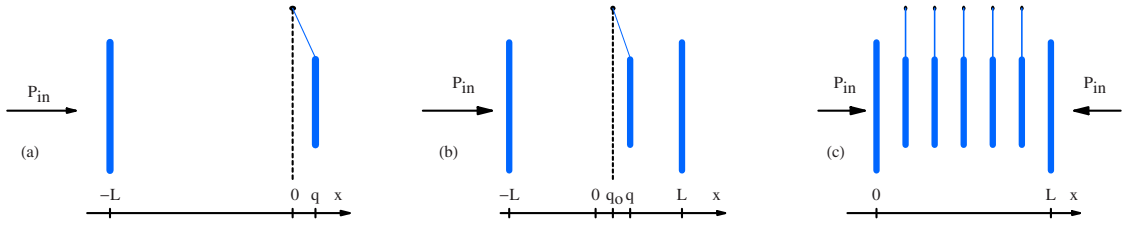

FIG. 1. (Color online). (a) The typical layout for optomechanical cooling and trapping using a two-mirror cavity (2MC). (b) A layout recently suggested by the authors for the same purpose using a three-mirror cavity (3MC) [6] with a perfectly reflecting middle mirror, and implemented experimentally in Ref. [7] using a partially transparent dielectric membrane in place of the middle mirror. In the proposal the 3MC was pumped from both sides; in the experiment the cavity was pumped from one side only, as shown in the figure. (c) A possible arrangement for scaling the technique to more than one mirror. The parameters labeling the figures are defined in the text.

In the 2MC the allowed laser power is limited by the onset of mirror bistability [10], placing bounds on the achievable cooling and trapping that can, however, be overcome by the implementation of feedback mechanisms [11]. In addition, in that geometry radiation pressure is not used optimally as it couples to the mirror from one side only, leading to an asymmetric optical potential [12].

Most importantly perhaps, the 2MC requires the movable mirror to be one of the end mirrors of a high finesse cavity and to have a high mechanical quality as well. Technically these are conflicting demands because the high finesse that maximizes the cooling effect of radiation is best achievable with massive, rigidly fixed mirrors. On the other hand, the high mechanical quality that minimizes the oscillator's coupling to thermal noise is best achievable with small, flexibly mounted mirrors. These opposing requirements represent the main experimental challenge to achieving states of vibration of low quantum number in the 2MC.

In a recent article we proposed an alternative geometry that allows one to reach and detect lower n_M's for comparable parameters [6] by suspending a perfectly reflecting mirror in the middle of a two-mirror cavity [Fig. 1(b)]. This three-mirror cavity (3MC) arrangement was shown to possess at least three advantages over the 2MC. First, it provides a higher value of ω_{eff} for the mirror [13–16], leading to fewer quanta of excitation, see Eq. (2). Second it removes bistability problems completely as far as the trapping fields are concerned, and partially for the cooling fields. Lastly, it increases the time available for observing the quantum dynamics of the mirror before the onset of thermal decoherence.

The present paper generalizes the analysis of the 3MC to the case where the middle mirror is partially transmitting. One major result is that in that case, the coupling of the mirror to the intracavity field can be either linear or quadratic in the mirror position. This has several important implications, including the possibility to measure an energy eigenstate of the mirror and also the possibility of developing novel mirror cooling methods. This is also a first step toward determining whether the same linear cavity can be used to quantize the motion of more than one mirror, see [Fig. 1(c)]. A classical treatment of the 3MC was presented earlier [13], however, the noise analysis did not include the vacuum fluctuations in the laser fields and ω_{eff} and D_{eff} were derived only in the static (zero-frequency) limit. Since we are concerned with cooling the movable mirror to its quantum mechanical ground state, a full quantized treatment is clearly needed. We derive expressions for the effective frequency and damping constant valid at any response frequency ω, and in making contact with the case of the perfectly reflecting middle mirror we include details that could not be presented in Ref. [6] because of lack of space.

In the course of concluding this work we became aware of a recent experiment that beautifully demonstrates the working of the 3MC and points out some of its additional virtues [7]. In that work Thompson *et al.* cooled a 50-nm-thick dielectric membrane placed inside an optical cavity from room temperature (294 K) down to 6.82 mK, i.e., by a factor of 4.4×10^4. These authors also pointed out that the 3MC solves a number of the technological challenges faced by the 2MC as it allocates the requirements of high optical finesse and high mechanical quality to different parts of the cavity [17]. The high finesse optical cavity now consists of two rigidly fixed mirrors, while the suspended middle mirror (or membrane) can independently have a high mechanical quality. Additionally in contrast to the 2MC that only allows the measurement of the mirror displacement q, the 3MC with mirrors of finite transmissivity allows in addition the measurement of q^2, thereby projecting the state of the mirror into an energy eigenstate [18].

Rather than elaborating on the salient features of Ref. [7], this paper examines the effect of middle-mirror transparency on the bistability, effective coupling to the light field, effective frequency, and damping displayed by the 3MC. In particular, the consideration of various limiting cases allows us to propose a two-color scheme that optimizes the cooling and trapping of the transparent mirror. We note that issues similar to those considered in this work have recently been addressed in Ref. [19] using a different formalism.

The paper is organized as follows. Section II derives a Hamiltonian of the moving mirror-cavity system valid in situations where it is sufficient to consider two modes of the cavity field, and Sec. III A shows how that Hamiltonian reduces to the case of a perfectly reflecting middle mirror [6]. We then turn to the case of a finite transmission, with Sec. III B discussing the situation when the moving mirror location yields a linear coupling to the photon number difference in the two field modes, and Sec. III C to the case where that coupling becomes quadratic. Section IV discusses the modification of the oscillation frequency and damping rate of the mirror by radiation pressure, Sec. V applies these results to the formulation of a proposal for a trapping and cooling configuration, and Sec. VI is a summary and conclusion. Appendix A contains a careful derivation of Eqs. (1) and (2), and Appendixes B and C present details of the cases considered in Secs. III B and III C.

II. MODEL HAMILTONIAN

We consider a 3MC geometry with the outer mirrors fixed at $x=\pm L$ [Fig. 1(b)] and a middle mirror of transmissivity T located at a position $x=q$. We assume the mirror thickness to be much smaller than an optical wavelength, a condition that has been realized experimentally [7].

A. Classical modes

We proceed by first determining the mode frequencies of the full resonator as a function of T and q. In the simple case $T=0$, $q=0$ the resonant frequencies of the two subcavities are

$$\omega_n = \frac{n\pi c}{L}, \tag{3}$$

where

$$n = 2L/\lambda_n, \tag{4}$$

$\lambda_n=2\pi c/\omega_n$, and n is the mode number (Table I).

When $T\neq0$, the two sides of the resonator are coupled and the modes of the complete system are found by solving

TABLE I. Definitions and approximate values of some of the parameters used in the text. These parameters lead to ground state occupation by the mirror. With more relaxed parameters low occupation numbers can still be reached. A proof-of-principle experiment has already been performed; for a description of the experiment and their parameters, see Ref. [7].

No.	Parameter	Description	Value	Units
1	L	subcavity length	5	mm
2	λ	laser wavelength	514	nm
3	n	mode number	10^4	
4	ω_n	cavity resonance frequency	$2\pi 10^{15}$	Hz
5	ξ	optomechanical coupling parameter	100	MHz nm^{-1}
6	ξ_L	linear optomechanical coupling	100	MHz nm^{-1}
7	T	middle mirror transmissivity	10^{-4}	
8	Δ_o	mode frequency shift	1	GHz
9	ξ_Q	quadratic optomechanical coupling	100	MHz nm^{-2}
10	m	middle mirror mass	1	μg
11	ω_M	middle mirror resonance frequency	$2\pi 2.5$	kHz
12	D_M	middle mirror damping constant	0.02	μg Hz
13	T_e	middle mirror initial temperature	300	K
14	T_{end}	end mirror transmissivity	10^{-5}	
15	γ	cavity linewidth	$2\pi 5$	MHz

the Helmholtz equation with the appropriate boundary conditions at $x=q, \pm L$, as described in Ref. [20]. For this calculation we assume for simplicity that the mirrors at $x = \pm L$ are perfectly reflecting. We also consider high-order cavity modes such that $L \gg \lambda_n$ and mirror displacements q (modulo λ_n) $\ll \lambda_n$. The finite transmission of the end mirrors will be accounted for later on.

Carrying through the classical calculation the wave vectors k supported by the full resonator appear as solutions to the transcendental Eq. [20]

$$\cot k(L+q) + \cot k(L-q) = 2\left(\frac{1-T}{T}\right)^{1/2}. \tag{5}$$

The solutions of Eq. (5) imply that as a result of the coupling between the two subcavities of the resonator each pair of initially twofold degenerate modes of frequency ω_n splits into a pair of nondegenerate modes, see Fig. 2,

$$\omega_{n,e}(q) \simeq \omega_n + \frac{1}{\tau}[\sin^{-1}(\sqrt{1-T}\cos 2k_n q) - \sin^{-1}(\sqrt{1-T})],$$

$$\omega_{n,o}(q) \simeq \omega_n + \frac{\pi}{\tau} - \frac{1}{\tau}[\sin^{-1}(\sqrt{1-T}\cos 2k_n q) + \sin^{-1}(\sqrt{1-T})], \tag{6}$$

where

$$\tau = 2L/c \tag{7}$$

is the round trip time for each subcavity, assumed to be approximately the same for both sides of the resonator for $L \gg \lambda_n$ and $q \ll \lambda_n$. In Eq. (6) $\omega_{n,e}$ corresponds to a mode with an even number of half wavelengths in the full resonator, while the mode at frequency $\omega_{n,o}$ has an additional half-wavelength, hence a slightly higher frequency. It corresponds to a field maximum at the center of the resonator, and turns into a "cosine" mode in the limit $T \to 1$, while the even mode of frequency $\omega_{n,e}$ turns into a "sine" mode in that limit. The electromagnetic fields corresponding to the frequencies in Eq. (6) can be found in Refs. [21,22]. In these references it is noted that due to the presence of a "dielectric bump" at the middle mirror the fields have a discontinuity in their derivative at that position. The cavity modes shown in Fig. 2 have been calculated and in addition experimentally detected in Ref. [7], justifying their use in the present article.

B. Quantization

Sections III and IV concentrate on an analysis restricted to the modes $\omega_{n,e}$ and $\omega_{n,o}$ about a specific ω_n (Table I). We

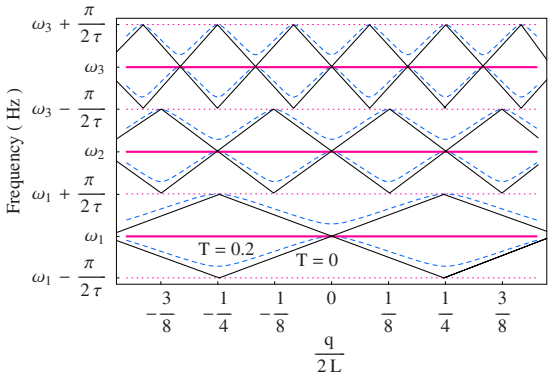

FIG. 2. (Color online). Numerical solution of Eq. (5) showing the eigenfrequencies ω_n of the full 3MC resonator [Fig. 1(b)] as a function of middle mirror position q. The solid black seesaw curves are for $T=0$ and the dashed blue sinusoidal curves are for $T=0.2$, chosen exaggeratedly for visibility.

quantize these two modes under the assumption that the oscillation frequency ω_M of the middle mirror is sufficiently small that $\tau \ll 1/\omega_M$, so that the electromagnetic field frequencies follow adiabatically the mirror motion, and $\omega_{n,e}(q)$ and $\omega_{n,o}(q)$ are simply parametrized by the mirror position q. Ignoring for notational simplicity the driving field, which will be introduced for particular pump configurations, the Hamiltonian of the coupled field-mirror system is then

$$H = \hbar\omega_e(q)a^\dagger a + \hbar\omega_o(q)b^\dagger b + \frac{p^2}{2m} + \frac{1}{2}m\omega_M^2(q-q_0)^2, \tag{8}$$

where we have dropped the subscript n for clarity, a and b are bosonic field operators for the modes of instantaneous frequencies ω_e and ω_o satisfying the commutation relations

$$[a,a^\dagger] = 1, \quad [b,b^\dagger] = 1, \tag{9}$$

p and q are the momentum and position operators of the moving mirror, with

$$[q,p] = i\hbar, \tag{10}$$

and q_0 is its rest position in the absence of radiation. The radiation pressure that couples the mirror motion to the resonator field is implicitly contained in the position dependence of ω_e and ω_o, see Eq. (6), as we will see shortly when considering various limits of the Hamiltonian [Eq. (8)].

III. TWO-MODE MODELS

A. Perfectly reflecting middle mirror

To set the stage for the discussion, we consider first the case of a perfectly reflecting middle mirror $T=0$, in which case the even and odd mode frequencies of Eqs. (6) reduce to the eigenfrequencies $\omega_{l,r}$ of the left and right subcavities of the 3MC

$$\omega_e = \omega_l \sim \omega_n(1-q/L), \quad \omega_o = \omega_r \sim \omega_n(1+q/L), \tag{11}$$

respectively. These frequencies are shown as the solid black seesaw lines in Fig. 2. For $q_0=0$ the Hamiltonian (8) can then readily be reexpressed (ignoring the pump fields) as

$$H = \hbar\omega_n(a^\dagger a + b^\dagger b) + \frac{p^2}{2m} + \frac{1}{2}m\omega_M^2 q^2 - \hbar\xi(a^\dagger a - b^\dagger b)q, \tag{12}$$

where

$$\xi = \omega_n/L \tag{13}$$

is the optomechanical coupling parameter and a and b are annihilation operators for the optical modes in the left and right subcavities [Fig. 1(c) in Ref. [6]]. In this form, the Hamiltonian (12) shows explicitly the effect of radiation pressure on the mirror motion. It is the form used in particular to discuss mirror cooling in Ref. [6]. We remind the reader that in this situation the cavity is optically pumped from both sides, in contrast to the pumping arrangement shown in Fig. 1(b).

We note that the Hamiltonian (12) also holds for $q_0 \neq 0$ after a trivial change of coordinate $q \to q - q_0$. Physically, this indicates that displacing the rest position of the moving mirror from the center of the resonator causes no qualitative change in its dynamics. In particular the radiation pressure term remains linear in the mirror position (again under the assumption that $q \ll \lambda_n$), and the cooling and trapping behavior is essentially the same as discussed in Ref. [6]. The situation is significantly different for the case $T \neq 0$, as we now discuss [23].

B. $T \neq 0$, linear coupling

As illustrated in Fig. 2, the coupling between the two subcavities resulting from the finite transmission of the moving mirror leads to the appearance of a series of avoided crossings between $\omega_e(q)$ and $\omega_o(q)$ near those points where either ω_n is doubly degenerate for $T=0$, or two frequencies $\omega_n(q)$ and $\omega_{n'}(q')$ become degenerate. The slopes of the solid seesaw lines in Fig. 2 are given by $\pm\omega_n/L = \pm n\pi c/L^2$ and are therefore n dependent, hence the anticrossing points are not equidistant. For large enough n, though, $n \simeq n+1$ and the avoided crossings occur for mirror separations $q \simeq l\bar{\lambda}/4$ from $q=0$, where l is an integer and $\bar{\lambda}$ is some typical wavelength about λ_n.

To lowest order, the dependence of $\omega_e(q)$ and $\omega_o(q)$ on q is linear away from the anticrossings, but quadratic in their vicinity. Hence we expect the radiation pressure contribution to the Hamiltonian (8) to be likewise linear and quadratic, respectively, in these two cases.

Consider first the linear case where $T \neq 0$ and the rest position q_0 of the moving mirror is away from any anticrossing point. For small enough mirror displacements $q \ll \bar{\lambda}$, we expand $\omega_e(q)$ and $\omega_o(q)$ about q_0 to find

$$\omega_e \sim \omega_n - \delta_e - \xi_L(q-q_0), \quad \omega_o \sim \omega_n + \delta_o + \xi_L(q-q_0), \tag{14}$$

where the frequency shifts are given by

$$\delta_e = \frac{1}{\tau}[\sin^{-1}(\sqrt{1-T}) - \sin^{-1}(\sqrt{1-T}\cos 2k_n q_0)], \tag{15}$$

$$\delta_o = \frac{\pi}{\tau} - \frac{1}{\tau}[\sin^{-1}(\sqrt{1-T}) + \sin^{-1}(\sqrt{1-T}\cos 2k_n q_0)], \tag{16}$$

and

$$\xi_L = \frac{\sin 2k_n q_0}{\sqrt{(1-T)^{-1} - \cos^2 2k_n q_0}}\xi \tag{17}$$

is a generalized linear optomechanical coupling parameter. It is easy to verify that $|\xi_L| \to \xi$ for $T=0$. When $T \neq 0$, $\xi_L = 0$ for $q_0 = j\lambda_n/4$, where j is an integer. This has important consequences that we discuss later on. A plot of ξ_L is given in Appendix C, Fig. 5.

With Eqs. (14) the Hamiltonian (8) becomes (ignoring the pump fields)

$$H = \hbar(\omega_n - \delta_e)a^\dagger a + \hbar(\omega_n + \delta_o)b^\dagger b + \frac{p^2}{2m} + \frac{1}{2}m\omega_M^2(q - q_0)^2 - \hbar\xi_L(a^\dagger a - b^\dagger b)(q - q_0) \quad (18)$$

or, with $q - q_0 \to q$,

$$H = \hbar(\omega_n - \delta_e)a^\dagger a + \hbar(\omega_n + \delta_o)b^\dagger b + \frac{p^2}{2m} + \frac{1}{2}m\omega_M^2 q^2 - \hbar\xi_L(a^\dagger a - b^\dagger b)q. \quad (19)$$

We note that writing this Hamiltonian is not equivalent to setting $q_0=0$, since Eq. (15) would then imply that $\xi_L=0$, and the radiation-mirror coupling would vanish.

Comparing Eqs. (12) and (19) shows that in the linear coupling regime, the finite mirror transmission results in the frequencies of the two modes $\omega_{e,o}$ being shifted by $-\delta_e$ and δ_o, respectively, and the optomechanical constant being redefined as $\xi \to \xi_L$. However, since the coupling of the radiation with the mirror remains linear there is no qualitative difference between the cooling and trapping mechanisms in the two cases.

Appendix C shows that a simple transformation can put the dynamical equations for the Hamiltonian Eq. (19) in a form identical to those for Eq. (12), with ξ replaced by ξ_L and $\delta_{e,o}$ absorbed as detuning shifts. In that same appendix we show that for an appropriate placement q_0 of the mirror we can obtain $\xi_L \sim \xi$. Hence it should be possible to trap and cool the partially transparent moving mirror to its quantum mechanical ground state with essentially the same parameters as the perfectly reflecting mirror [6]. In Table I we present such a set of parameters. Another set of parameters has been suggested in Ref [7].

C. $T \neq 0$, quadratic coupling

We now turn to the situation where the middle mirror is placed at a position $q_0 = j\lambda_n/4$ (j integer). In that case, expanding Eqs. (6) to lowest order about q_0 gives

$$\omega_e \sim \omega_n - \xi_Q(q - q_0)^2, \quad \omega_o \sim \omega_n + \Delta_o + \xi_Q(q - q_0)^2, \quad (20)$$

where the detuning is given by

$$\Delta_o = \frac{2}{\tau}\cos^{-1}(1 - T)^{1/2} \quad (21)$$

and the quadratic optomechanical coupling constant is

$$\xi_Q = \frac{\tau\xi^2}{2}\left(\frac{1 - T}{T}\right)^{1/2}. \quad (22)$$

The detuning Δ_o and ξ_Q are plotted in Fig. 3 as functions of T. The Hamiltonian (8) now becomes (ignoring the pump fields)

$$H = \hbar\omega_n a^\dagger a + \hbar(\omega_n + \Delta_o)b^\dagger b + \frac{p^2}{2m} + \frac{1}{2}m\omega_M^2(q - q_0)^2 - \hbar\xi_Q(a^\dagger a - b^\dagger b)(q - q_0)^2. \quad (23)$$

Since Δ_o and ξ_Q are independent of q_0 we can rescale that Hamiltonian by the transformation $q - q_0 \to q$ without affecting any of the physics. This is equivalent to setting $q_0=0$ and yields

$$H = \hbar\omega_n a^\dagger a + \hbar(\omega_n + \Delta_o)b^\dagger b + \frac{p^2}{2m} + \frac{1}{2}m\omega_M^2 q^2 - \hbar\xi_Q(a^\dagger a - b^\dagger b)q^2. \quad (24)$$

As expected from our previous discussion, the mirror-radiation coupling is now quadratic in the mirror coordinate, in contrast to Eqs. (12) and (19), where it is linear [7]. This coupling is purely dispersive and leads to qualitatively different radiation effects. We show below that such a coupling implies in particular the ability to trap but not cool the moving mirror.

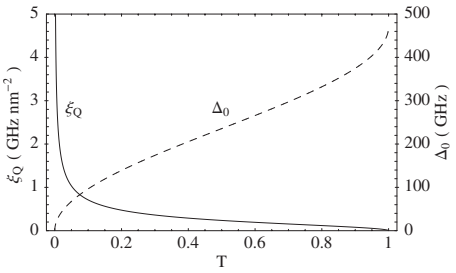

FIG. 3. Detuning Δ_o (dotted line) [Eq. (21)] and quadratic optomechanical coupling constant ξ_Q (solid line) [Eq. (22)] as functions of the middle mirror transmissivity T. The parameter values used to generate these plots are provided in Table I.

IV. QUADRATIC COUPLING-EFFECTIVE FREQUENCY AND DAMPING

A. Quantum Langevin equations

We consider for concreteness a simple implementation of the 3MC trapping and cooling scheme where the system is driven by a narrow-band laser field of frequency ω_L impinging on the resonator from the left, the right end-mirror being assumed to be perfectly reflecting, as shown in Fig. 1(b). As previously discussed [5], in the case of linear coupling two lasers of different frequencies have to be used in practice to control the moving mirror. Except for the fact that the powers and frequencies of these two fields must be chosen self-consistently in order to ensure the dynamic stability of the system, one of them essentially affects solely the spring frequency and the other only the spring damping. This case is reviewed in Appendix B, which also makes contact with the situation of a perfectly reflecting middle mirror.

In this section we consider instead the case of quadratic coupling and show that in that regime the damping constant of the moving mirror remains unchanged from its intrinsic value. The differences in the physics governing the cases of linear and quadratic coupling is further discussed in Sec. IV E. At this point we introduce an additional simplification by noting that for the value of T considered here we have $\Delta_o \gg \gamma$ (Table I), that is, the frequency separation of the two modes is much larger than the cavity linewidth. In that case, and provided that the laser linewidth is comparable to or less

than γ, it is sufficient to consider a single-mode treatment that involves only the resonator mode closest to ω_L. Single-mode coupling of a laser to either mode has been demonstrated experimentally in the case where both end mirrors are slightly transparent, justifying our assumptions [7].

By inspection of the last term in Eq. (24) we expect that the "a" mode will cause antitrapping since it is associated with a negative "spring constant" $-\hbar\xi_Q a^\dagger a$ while the mode "b" should lead to mirror trapping. Moreover we expect the modification to the trapping frequency to be a maximum when the photon number (intracavity intensity) in the mode reaches a maximum. For a given laser power this should happen, as we will confirm later, at zero detuning, i.e., on resonance. Tuning the laser close to the frequency of the mode b yields then the approximate single-mode Hamiltonian (ignoring the pump fields)

$$H \simeq \hbar(\omega_n + \Delta_o)b^\dagger b + \frac{p^2}{2m} + \frac{1}{2}m\omega_M^2 q^2 + \hbar\xi_Q b^\dagger b q^2, \quad (25)$$

which we analyze below.

The fluctuations of the electromagnetic vacuum couple into the resonator through the partially transmitting input mirror, which also leads to the damping of the intracavity field. Further, the Brownian noise associated with the coupling of the oscillating mirror to its thermal environment must be accounted for in a realistic treatment of the mirror dynamics. We describe the effect of these sources of noise and dissipation within the input-output formalism of quantum optics [24]. For the Hamiltonian (25) this yields in a standard fashion the nonlinear quantum Langevin equations [25]

$$\dot{b} = -\left[i(\delta + \xi_Q q^2) + \frac{\gamma}{2}\right]b + \sqrt{\gamma}b^{\text{in}}, \quad \dot{q} = \frac{p}{m},$$

$$\dot{p} = -(2\hbar\xi_Q b^\dagger b + m\omega_M^2)q - \frac{D_M}{m}p + \epsilon^{\text{in}}, \quad (26)$$

where the detuning is given by

$$\delta = \omega_n + \Delta_o - \omega_L \quad (27)$$

and

$$\gamma = \frac{cT_{\text{end}}}{2L} \quad (28)$$

is the decay rate through the input mirror of transmissivity T_{end} (Table I). We remind the reader that we are considering left-sided pumping of the 3MC, and the mirror at the right end is considered to be perfectly reflecting.

In Eq. (26) the noise operator b^{in} describes the field pumping the cavity mode. It is characterized by the semiclassical mean value

$$\langle b^{\text{in}}(t)\rangle = b_s^{\text{in}} \quad (29)$$

and Markovian fluctuations

$$\langle \delta b^{\text{in}}(t)\delta b^{\text{in},\dagger}(t')\rangle = \delta(t-t'). \quad (30)$$

The Brownian noise operator ϵ^{in} describes the heating of the mirror by its thermal environment. It is characterized by a zero mean value, and fluctuations at temperature T_e correlated as [24]

$$\langle \delta\epsilon^{\text{in}}(t)\delta\epsilon^{\text{in}}(t')\rangle = D_M \int_{-\infty}^{\infty} \frac{d\omega}{2\pi} e^{-i\omega(t-t')}\hbar\omega\left[1 + \coth\left(\frac{\hbar\omega}{2k_B T_e}\right)\right]. \quad (31)$$

For the parameters of our model, $T_e \gg \hbar\omega_{\text{eff}}/k_B$, and therefore the high-temperature limit of Eq. (31)

$$\langle \delta\epsilon^{\text{in}}(t)\delta\epsilon^{\text{in}}(t')\rangle = 2D_M k_B T_e \delta(t-t') \quad (32)$$

is applicable.

B. Steady state

Appendix C shows that for any value of ξ_Q, $q_s=0$ is the only real steady-state solution for the mirror displacement. In contrast to standard configurations bistability does not occur because we have chosen a trapping mode for the mirror. The steady-state of the mirror-cavity system is given by

$$q_s = 0, \quad p_s = 0, \quad b_s = \left[\frac{\gamma}{\delta^2 + (\gamma/2)^2}\right]^{1/2} f_s^{\text{in}}, \quad (33)$$

where $f_s^{\text{in}} = |b_s^{\text{in}}|$ is the amplitude of the laser field pumping the cavity. The phase of this field can be chosen without loss of generality such that b_s is real. The steady-state intracavity field mode amplitude b_s in Eq. (33) is independent of ξ_Q, a consequence of the fact that $q_s=0$.

C. Fluctuations

To account for the effect of the classical and quantum fluctuations we decompose each operator in Eq. (26) as the sum of its steady-state value and a small fluctuation, e.g., $b = b_s + \delta b$. Substituting these quantities into Eq. (26), eliminating the steady-state contribution and linearizing the resulting equations for the fluctuations we have

$$\dot{u}(t) = Mu(t) + n(t). \quad (34)$$

Here the vectors of the input noise and fluctuations are, respectively, given by

$$u(t) = (\delta X_b, \delta Y_b, \delta q, \delta p), \quad n(t) = (\sqrt{\gamma}X_b^{\text{in}}, \sqrt{\gamma}Y_b^{\text{in}}, 0, \delta\epsilon^{\text{in}}), \quad (35)$$

and we have symmetrized the fluctuation operators as $\delta X_b = (\delta b + \delta b^\dagger)/\sqrt{2}$, $\delta Y_b = (\delta b - \delta b^\dagger)/i\sqrt{2}$, etc. The matrix M is given explicitly by

$$M = \begin{pmatrix} -\gamma/2 & \delta & 0 & 0 \\ -\delta & -\gamma/2 & 0 & 0 \\ 0 & 0 & 0 & 1/m \\ 0 & 0 & -(2\hbar\xi_Q b_s^2 + m\omega_M^2) & -D_M/m \end{pmatrix}. \quad (36)$$

The steady-state solutions (33) are dynamically stable if none of the eigenvalues of the matrix M has a positive real part. This condition can be quantified in terms of the Routh-

Hurwitz criterion [26], which yields inequalities too involved to be presented here. However, we will work at $\delta=0$ in the following and it is quite easy to show analytically that for this detuning and any value of the other parameters of Eq. (36) there is no dynamical instability in the 3MC.

D. Effective frequency and damping

In order to determine the effective frequency $\omega_{\rm eff}$ and damping $D_{\rm eff}$ of the mirror in the regime of quadratic coupling (25), we solve the linearized quantum Langevin equations for the fluctuations in the mirror position

$$\delta q(\omega) = \chi(\omega)\delta F_T(\omega), \tag{37}$$

where $\chi(\omega)$ is the mechanical susceptibility of the mirror and δF_T, which describes the fluctuations in the total force on the mirror, consists of a radiation vacuum and a Brownian motion component. The susceptibility has the form of a Lorentzian [27]

$$\chi^{-1}(\omega) = m(\omega_{\rm eff}^2 - \omega^2) - iD_{\rm eff}\omega, \tag{38}$$

from which we can extract the effective oscillation frequency $\omega_{\rm eff}$ and damping constant $D_{\rm eff}$ of the mirror as

$$\omega_{\rm eff}^2 = \omega_M^2 + \frac{(2\xi_Q\gamma P_{\rm in}/m\omega_n)}{\delta^2 + (\gamma/2)^2}, \quad D_{\rm eff} = D_M, \tag{39}$$

where $P_{\rm in}=\hbar\omega_n|f_s^{\rm in}|^2$ is the input power of the incident laser.

The results displayed in Eq. (39) are striking for a number of reasons. First, we note that $D_{\rm eff}$ is unchanged from its intrinsic value. Second, neither $\omega_{\rm eff}$ nor $D_{\rm eff}$ depend on the system response frequency ω, in contrast to the results of the linear coupling theory [Eq. (B3)]. Third, from the expression for $\omega_{\rm eff}$ in Eq. (39) we see that the trapping effect of the mode is maximized on resonance and is symmetric about it, in contrast to the usual optomechanical result where no trapping is possible on resonance, optimum trapping occurs when the laser is blue-detuned and antitrapping occurs when the laser is detuned to the red of the cavity resonance.

Before we discuss these differences in detail in the following section we note that following Eq. (39) it can be concluded that the mirror can be optically trapped by selectively exciting the mode $\omega_{\rm o}$, and that the trapping effect is strongest on resonance $\delta=0$, with the resulting trapping frequency given by

$$\omega_{\rm max}^2 = \omega_M^2 + \frac{4\xi_Q P_{\rm in}}{m\omega_n\gamma}. \tag{40}$$

Also, unlike usual optomechanical trapping [Eq. (B3)] which degrades at high frequencies ($\omega \gg \gamma$), the effective frequency in Eq. (39) is independent of ω and is the same for all mirrors of equal mass and transparency. Further, for this configuration there is neither (static) bistability nor dynamical instability (Appendix C), hence a high laser power can be used to achieve tight mirror traps, limited only by the effects of mirror heating.

In Eq. (39) the effective frequency depends on the mirror transmissivity through the coupling parameter ξ_Q [Eq. (22)], which can vary with T as evident from Fig. 3. For the parameters of this paper the effective frequency $\omega_{\rm eff}$ turns out to be much larger than the bare mechanical frequency ω_M (see below) and it is comparable to the effective frequency achieved in the 3MC with a perfectly reflecting middle mirror [Eq. (7) in Ref. [6]]. However, the trapping light does not introduce any antidamping in the present case, in contrast to the linear coupling regime.

For completeness we mention that an equivalent single-mode treatment of the coupling of the incident laser into the even mode of frequency ω_e leads to antitrapping and instabilities, both static as well as dynamic. We do not consider this regime further in this paper.

E. Discussion

This section presents a qualitative discussion of the physics underlying the linear and quadratic cooling and trapping effects. Specifically we show that the mechanisms behind the optomechanical effects are different in the two cases, leading to a ω dependence of the effective parameters in the linear case and ω independence in the quadratic case. In addition we explain the absence of damping and the presence of trapping in the case of the quadratic coupling.

It is known that in the case of linear optomechanical coupling mirror trapping and cooling are enabled by the mechanism of cavity back-action [1–5]. Back-action results from the fact that the motion of the mirror modifies the frequency of the cavity mode. In turn, this changes the optical power inside the cavity, which now exerts a different pressure on the mirror than before. Back-action becomes important when the storage time of the light in the cavity (γ^{-1}) becomes comparable to the oscillation frequency of the moving end mirror. The delay time associated with back-action reveals itself in the ω dependence of the effective parameters [Eq. (B3)]. This implies that back-action effects are absent in the case of quadratic coupling [Eq. (39)], since there is no ω dependence. This explains why the damping is not changed from its bare value in that case and suggests also that the trapping is not due to a back-action mechanism.

In order for back-action to work there also has to be an asymmetry in the way the cavity frequency changes for the two directions of mirror motion: displacements to the right have to lead away from the cavity resonance while displacements to the left have to lead toward it, or the opposite (the selection can be made by detuning the laser frequency appropriately). This ensures that the power in the cavity increases for one direction of mirror motion and decreases for the opposite direction, so that the radiation supplies the "negative feedback" to the mirror motion that leads to trapping and damping. In the simplest case this is realized if the cavity resonance is a linear function of the mirror position. However, if the change in the cavity mode frequency is symmetric in the mirror position as is the case for quadratic coupling, then the back-action cannot cause trapping or damping as it always results in the same force on the mirror, regardless of its direction of motion. This explains the ω independence of the effective parameters for the quadratic coupling case as well as the absence of associated optical damping effects [Eq. (39)].

It remains to explain the trapping effect of the quadratic coupling [Eq. (39)]. This can be done simply by realizing that the presence of the resonator modifies the potential seen by the oscillating mirror. Here, radiation pressure trapping translates into an increase in the effective mirror frequency from its "bare" value ω_M as follows. From elementary mechanics we know that a perturbation to the harmonic oscillator that is quadratic in its position q merely serves to modify its frequency. Specifically, the term $-\hbar\xi_Q a^\dagger a q^2$ decreases the mirror frequency (antitrapping), while the term $\hbar\xi_Q b^\dagger b q^2$ increases it (trapping). Since the intracavity light intensity is maximized on resonance, so is the effective frequency.

While discussing the effects of intracavity intensity, it is relevant to ask how the mirror dynamics are influenced by the balance of power in either subcavity of the 3MC. In particular we would like to find out if the trapping action of the radiation can be simply thought of in terms of the amount of radiation contained in the two halves of the 3MC. In the case of linear coupling, the intensity balance between the two subcavities turns out not to affect ω_{eff}. Perhaps the simplest way to see that is by considering the 2MC where for the same intracavity intensity trapping can occur for blue-detuning of the laser while antitrapping occurs for red-detuning.

On the other hand, in the case of quadratic coupling the power balance between the two subcavities leads to a further understanding of the trapping effect. From the details of the classical electromagnetic analysis of Sec. II A it is possible to determine the electric field amplitude E_k for each eigenmode k [given by Eq. (5)] of the 3MC. In particular the ratio I_r of the intensities of the component of E_k in the right and left subcavities turns out to be [21]

$$I_r = \left(\frac{\sin[k(L+q)]}{\sin[k(L-q)]}\right)^2, \\ = 1 + 2k\cot(kL)q + \cdots, \tag{41}$$

the second line being an expansion for small mirror displacements q.

It is clear from the first line of Eq. (41) that if the mirror is exactly in the middle of the cavity ($q=0$), then the field intensities in the two subcavities are identically equal ($I_r=1$). An analysis of the second line yields the following intuition, which is confirmed by a full numerical evaluation. For an odd mode, such as b, kL is a little more than an integer multiple of π (Fig. 2). This implies $\cot(kL)>0$. Hence, if the mirror moves slightly to the left ($q<0$) then the intensity in the left cavity becomes larger than that in the right [21] ($I_r<1$). Likewise when the mirror moves to the right, the right cavity hosts more power ($I_r>1$). This provides a classical picture of trapping in the regime of quadratic optomechanical coupling. On the other hand, for an even mode such as a, the opposite is true. The value of kL is a little less than an integer multiple of π (Fig. 2) and $\cot(kL)<0$. If the mirror moves to the right, for example, the left subcavity intensity becomes larger than the right. The presence of antitrapping for the even mode follows from this description. We note that the position and the transmissivity of the middle mirror completely determine the ratio I_r, so that the side from which the 3MC is pumped is irrelevant.

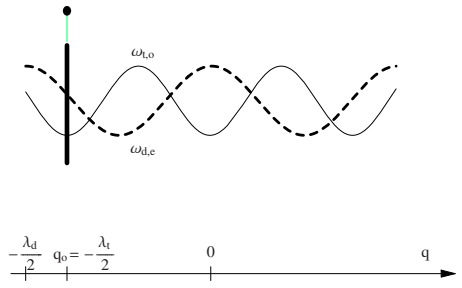

FIG. 4. (Color online) Schematics of the two-color cooling and trapping scheme. The region close to the center of the cavity ($q=0$) is shown. The sinusoidal curves correspond to the frequencies of two resonator modes as a function of the middle mirror displacement q from the origin. An odd mode of frequency $\omega_{t,o}$ (solid line) excited by a laser of wavelength λ_t and an even mode of frequency $\omega_{d,e}$ (dotted line) excited by a second laser of wavelength λ_d are shown. The equilibrium position q_0 of the mirror is chosen so as to coincide with a minimum of the $\omega_{t,o}$ mode and to be slightly to the right of a maximum of the $\omega_{d,e}$ mode. Red-detuning the wavelength λ_d of the second laser damps the mirror motion via a linear optomechanical coupling and tuning the wavelength λ_t of the trapping field to resonance traps the mirror via a quadratic optomechanical coupling.

The case of the quadratic coupling is purely dispersive, as pointed out in Ref. [7]. Such effects resemble the Stark shifts of the levels of an atom interacting with a single light mode in a cavity [28]. In the dispersive limit the atom acts as a small dielectric similar to the mirror in the middle of the 3MC; changes in the cavity resonance frequencies may be thought of as being due to the "atomic index." Similar effects have been predicted to occur in solid state systems [29] and have recently been observed [30].

V. BICHROMATIC TRAPPING AND COOLING

Summarizing our results so far, we have shown in Sec. III B and Appendix B that in the regime of linear optomechanical coupling an even mode can be used to achieve passive cooling, while Sec. IV D demonstrates the possibility of achieving a large effective frequency ω_{eff} without introducing any antidamping in the regime of quadratic optomechanical coupling by using an odd mode. These results suggest the use of two incident lasers at wavelengths λ_d and λ_t that drive the mirror in the linear and quadratic coupling regimes, respectively, to damp and trap its motion, see Fig. 4. These wavelengths are chosen such that the corresponding resonant cavity mode numbers $n_{d,t} \gg 1$ so that $n_{d,t} \sim n_{d,t}+1$. We also assume that each incident laser is effectively coupled to only one cavity mode so that the single-mode treatments of Secs. IV D and III B and Appendix B are valid. In order for the two lasers to act essentially independently on the moving mirror we also require that they couple into resonator modes whose frequency separation is much larger than γ.

The dependence of the frequencies $\omega_{t,o}$ and $\omega_{d,e}$ of the two relevant cavity modes on the mirror position q is as

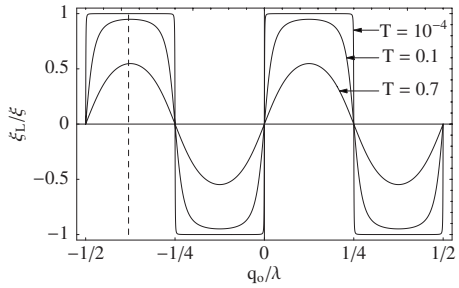

FIG. 5. Linear optomechanical coupling parameter ξ_L as a function of the middle mirror placement q_0 for various values of the mirror transmission T. The dotted line indicates the position of the mirror at $q_0=-\lambda/2+\lambda/10$, allowing ξ_L to approach closely the maximum value ξ corresponding to a perfectly reflecting mirror.

illustrated in Fig. 2, but with the mutual shift in position shown schematically in Fig. 4. The moving mirror is at a position such that $\omega_{t,o}$ has an extremum (the first minimum to the left of $q=0$, at $q_0=-\lambda_t/2$ in Fig. 4). The laser excitation of that mode results in mirror trapping with no antidamping, as we have seen.

The first maximum of $\omega_{d,e}$ is at $-\lambda_d/2$ from the cavity center, hence the mirror is at a distance $(\lambda_d-\lambda_t)/2$ to the right of that maximum, see Fig. 4. Appendix B shows that regular passive cooling can be implemented by red-detuning the λ_d radiation from $\omega_{d,e}$, and that in order to optimize radiation effects for $T\sim 10^{-4}$ the mirror should be displaced by an amount of the order of $\lambda_d/10$ to the right of the maximum of $\omega_{d,e}$, (Fig. 5). This implies

$$(\lambda_d-\lambda_t)/2=\lambda_d/10, \tag{42}$$

which gives $\lambda_t=0.8\lambda_d$ for the example of Fig. 4. In an actual experiment, an appropriate q_0 can be found empirically given two available laser wavelengths.

This "hybrid" configuration enables a trap stiffness unrestricted by considerations of antidamping. In other words the trapping light at λ_t does not destabilize or raise the noise temperature of the middle mirror at all. This technique is therefore superior to the standard trapping and cooling scheme based only on a radiation-mirror-coupling linear in the mirror coordinate, such as Eqs. (12) or (19). Both the effective mirror damping (due to absence of antidamping) as well as the mirror trapping (due to absence of instabilities) can be stronger in the hybrid case, and the achievable final degree of vibrational excitation [Eq. (2)] is therefore lower.

For example, if antidamping is absent in the case of purely linear coupling treated in Appendix B, the total damping increases by a factor of $\sim$100, implying a mirror temperature lower by the same factor. The trapping required to reach the ground state now can be achieved by 8 mW of laser light on resonance.

VI. CONCLUSION

The radiative trapping and cooling of a totally and partially reflecting mirror in an optical cavity has been considered theoretically. Our main conclusion is that allowing the middle mirror to be transmissive does not greatly affect the ability of radiation to cool the mirror down to its quantum mechanical ground state. However, it leads to the possibility of changing the coupling between the mirror and the intracavity field from linear to quadratic in the mirror displacement, depending on the position of the middle mirror with respect to the end mirrors of the cavity. This is in agreement with the analysis of Ref. [7]. One important point is that in the dispersive regime it is possible to achieve a strong optical trapping of the mirror without the addition of any antidamping. However, the physical mechanism behind this trapping is not the usual back-action-induced effect observed in standard optomechanical experiments.

Combining the various regimes of optomechanical coupling, we have also proposed a two-color mirror trapping and cooling scheme based on positioning the mirror so as to simultaneously couple it dissipatively with one cavity mode and dispersively with a second mode. In contrast to all the configurations implemented or discussed in the literature so far, trapping in this configuration does not cause antidamping or instabilities of either the static or dynamic kind. This improves the damping effect of radiation while allowing for tighter mirror traps to be established using higher laser power. This allows one to reach lower mirror temperatures and eases the route to the occupation of the quantum mechanical ground state of the moving mirror.

ACKNOWLEDGMENTS

This work is supported in part by the U.S. Office of Naval Research, by the National Science Foundation, and by the U.S. Army Research Office. We thank O. Dutta, Dr. C. Maes, and Professor H. Ritsch for useful discussions.

APPENDIX A: EFFECTIVE TEMPERATURE AND QUANTA

This appendix derives Eqs. (1) and (2) and discusses their limit of validity. We mention here a correction to Eq. (1) of Ref. [6], which presented an incorrect scaling of the mirror quanta with effective frequency, and thus underestimated the degree of excitation of the mirror. This correction, however, does not bring any qualitative change to our previous results [6]. That same correction has recently been realized by other authors [8,9].

The starting point of our derivation is Eq. (37). For the parameters of the model discussed in Secs. III A, III B, and III C, the fluctuations in the total force are due mainly to thermal noise, so that $\delta F_T(\omega)\sim\delta\epsilon^{\rm in}(\omega)$. In the case of Sec. III C this is exactly true, i.e., $\delta F_T(\omega)\equiv\delta\epsilon^{\rm in}(\omega)$ since fluctuations in the radiation field do not couple to the mirror motion in the framework of linear response theory. In either case the two-time correlation function of the force fluctuations is therefore that of the thermal component

$$\langle\delta F_T(t)\delta F_T(t')\rangle=\langle\delta\epsilon^{\rm in}(t)\delta\epsilon^{\rm in}(t')\rangle=N\delta(t-t'), \tag{A1}$$

where $N=2D_Mk_BT_e$ according to Eq. (32).

Fourier transforming (FT) both sides of Eq. (A1) using the symmetric FT

$$\delta F_T(\omega) = \frac{1}{\sqrt{2\pi}} \int_{-\infty}^{\infty} dt \; e^{i\omega t} \delta F_T(t) \tag{A2}$$

gives the frequency-domain correlation function

$$\langle \delta F_T(\omega) \delta F_T(\omega') \rangle = N \delta(\omega + \omega'), \tag{A3}$$

which in turn allows us to express the correlation function for the linear displacement, see Eq. (37), as

$$\langle \delta q(\omega) \delta q(\omega') \rangle = N \chi(\omega) \chi(\omega') \delta(\omega + \omega'). \tag{A4}$$

Inverse Fourier transforming both sides of Eq. (A4) we get

$$\langle \delta q(t) \delta q(t') \rangle = \frac{N}{2\pi} \int_{-\infty}^{\infty} d\omega \; e^{-i\omega(t-t')} |\chi(\omega)|^2, \tag{A5}$$

since $\chi(-\omega) = \chi^*(\omega)$ from Eqs. (38), (39), and (B3). Setting $t = t'$ in Eq. (A5) we get

$$\langle \delta q^2(t) \rangle = \frac{N}{2\pi} \int_{-\infty}^{\infty} d\omega |\chi(\omega)|^2. \tag{A6}$$

We now use the equipartition theorem to link the average displacement squared to T_{eff}, the effective temperature of the vibrating mirror

$$\frac{k_B T_{\text{eff}}}{2} = \frac{m \omega_{\text{eff}}^2 \langle \delta q^2(t) \rangle}{2}. \tag{A7}$$

Note that the equipartition theorem is expressed in terms of the effective frequency of the mirror. Combining Eqs. (A6) and (A7) we find

$$T_{\text{eff}} = T_e \left(\frac{m \omega_{\text{eff}}^2 D_M}{\pi} \right) \int_{-\infty}^{\infty} d\omega |\chi(\omega)|^2. \tag{A8}$$

This allows us to determine the mean number of quanta of vibration of the moving mirror as

$$n_M = \frac{k_B T_{\text{eff}}}{\hbar \omega_{\text{eff}}} = \frac{k_B T_e}{\hbar} \left(\frac{m \omega_{\text{eff}} D_M}{\pi} \right) \int_{-\infty}^{\infty} d\omega |\chi(\omega)|^2, \tag{A9}$$

where

$$\chi^{-1}(\omega) = m[\omega_{\text{eff}}^2(\omega) - \omega^2] - i D_{\text{eff}}(\omega) \omega. \tag{A10}$$

The exact form of the effective frequency and damping depend on the position and transmission of the middle mirror. They are given by either Eq. (39) or Eq. (B3). In the case of Eq. (39) the effective quantities do not depend on ω. In the case of Eq. (B3) we expand them in a Taylor series around $\omega = \omega_M$ and keep only the leading terms in the respective expansions (see below for justification),

$$\omega_{\text{eff}}^2(\omega) \sim \omega_{\text{eff}}^2(\omega_M) \equiv \omega_{\text{eff}}^2, \quad D_{\text{eff}}(\omega) \sim D_{\text{eff}}(\omega_M) \equiv D_{\text{eff}}. \tag{A11}$$

With Eq. (A11) we find analytically

$$\int_{-\infty}^{\infty} d\omega |\chi(\omega)|^2 = \frac{\pi}{m(\omega_{\text{eff}})^2 D_{\text{eff}}}. \tag{A12}$$

Equations (A8) and (A9) then imply

$$T_{\text{eff}} = \left(\frac{D_M}{D_{\text{eff}}} \right) T_e \tag{A13}$$

and

$$n_M = \frac{k_B T_{\text{eff}}}{\hbar \omega_{\text{eff}}} = \frac{k_B T_e}{\hbar \omega_{\text{eff}}} \left(\frac{D_M}{D_{\text{eff}}} \right), \tag{A14}$$

respectively. These are precisely Eqs. (1) and (2). Evidently Eqs. (A12)–(A14) are exact when the effective frequency and damping follow from Eq. (39). (We will say no more about this case.) These results are, however, approximate when the effective frequency and damping follow from Eq. (B3).

To ensure that the approximation stated in Eq. (A11) is accurate, we used the full functional forms of $\omega_{\text{eff}}(\omega)$ and $D_{\text{eff}}(\omega)$ from Eq. (B3), and performed the integral in Eq. (A12) numerically. For the parameters used in this paper this yields numerical values indistinguishable from the approximate analytical expressions, i.e., we found the same effective temperature and quanta for the mirror.

The condition that needs to be satisfied for the approximation in Eq. (A11) to be valid can be found by inspecting the forms of the functions $\omega_{\text{eff}}(\omega)$ and $D_{\text{eff}}(\omega)$ in Eq. (B3). Expanding analytically these expressions in Taylor series about ω_M and defining

$$V = \frac{4\xi\gamma P_{\text{in}}}{mL}, \tag{A15}$$

we find

$$\omega_{\text{eff}}^2(\omega) = \omega_{\text{eff}}^2(\omega_M) + d(\omega_M)(\omega - \omega_M) + O[(\omega - \omega_M)^2], \tag{A16}$$

where

$$\omega_{\text{eff}}^2(\omega_M) = \omega_M^2 - \frac{16V\delta(-4\omega_M^2 + \gamma^2 + 4\delta^2)}{(\gamma^2 + 4\delta^2)[16\omega_M^4 + 8\omega_M^2(\gamma^2 - 4\delta^2) + (\gamma^2 + 4\delta^2)^2]} \simeq - \frac{16V\delta(-4\omega_M^2 + \gamma^2 + 4\delta^2)}{(\gamma^2 + 4\delta^2)[16\omega_M^4 + 8\omega_M^2(\gamma^2 - 4\delta^2) + (\gamma^2 + 4\delta^2)^2]} \tag{A17}$$

is the first term in the expansion and ω_M^2 can be neglected since we are in a regime where the optical contribution to the stiffness is typically much larger than the intrinsic mechanical contribution [this may be translated into an appropriate condition on V, Eq. (A15)]. The coefficient of the second term in Eq. (A16) is

$$d(\omega_M) = \frac{-128V\omega_M\delta[16\omega_M^4 - 3\gamma^4 - 8\gamma^2\delta^2 + 16\delta^4 - 8\omega_M^2(\gamma^2 + 4\delta^2)]}{(\gamma^2 + 4\delta^2)[16\omega_M^4 + 8\omega_M^2(\gamma^2 - 4\delta^2) + (\gamma^2 + 4\delta^2)^2]^2}. \tag{A18}$$

The contribution of the second term becomes comparable to that of the first in Eq. (A16) at the critical frequency

$$\omega_{\rm crit} = \omega_M - \frac{(4\omega_M^2 - \gamma^2 - 4\delta^2)[16\omega_M^4 + 8\omega_M^2(\gamma^2 - 4\delta^2) + (\gamma^2 + 4\delta^2)^2]}{8\omega_M[16\omega_M^4 - 3\gamma^4 - 8\gamma^2\delta^2 + 16\delta^4 - 8\omega_M^2(\gamma^2 + 4\delta^2)]}. \tag{A19}$$

Using the hierarchy $\delta \geq \gamma/2 \gg \omega_M$ applicable to this article, we approximate Eq. (A19) and get

$$\omega_{\rm crit} \simeq \omega_M\left[1 + \frac{1}{2}\left(\frac{\delta}{\omega_M}\right)^2\right]. \tag{A20}$$

The detuning is usually a few cavity linewidths for trapping, e.g., $\delta = -2.5\gamma$ in this work. Thus $\delta/\omega_M \sim 10^3$ and therefore $\omega_{\rm crit} \sim 10^6\omega_M$. Also, for our parameters $\omega_{\rm eff}(\omega_M) \lesssim 10^3\omega_M$. This implies that not only is the critical frequency much larger than the intrinsic mechanical frequency, it is also much larger than the optically induced mirror frequency, an important observation. A similar result can be obtained for $D_{\rm eff}$, in which case $\delta = \gamma/2$. The general conclusion is that for our parameters the higher-order frequency-dependent terms in the expansions of $\omega_{\rm eff}(\omega)$ and $D_{\rm eff}(\omega)$ become important at frequencies much higher than $\omega_{\rm eff}(\omega_M)$.

Now for $\omega_{\rm eff}(\omega) \simeq \omega_{\rm eff}(\omega_M)$ [from Eq. (A11)] the integrand in Eq. (A8) is a Lorentzian peaked at $\omega_{\rm eff}(\omega_M)$, with a symmetric peak at $-\omega_{\rm eff}(\omega_M)$. The regime $|\omega| \geq \omega_{\rm crit}$ then corresponds to the far-out wings of the Lorentzian, since $\omega_{\rm crit} \gg \omega_{\rm eff}(\omega_M)$. In this regime the contribution of the higher-order terms to the spectrum is highly suppressed, resulting in virtually no change in the area underneath the spectrum and no change in the scalings in Eqs. (A13) and (A14). Thus the condition under which Eqs. (1) and (2) hold is

$$\omega_{\rm eff}(\omega_M) \ll \omega_{\rm crit}, \tag{A21}$$

which is well satisfied in our case.

APPENDIX B: LINEAR OPTOMECHANICAL COUPLING

This appendix discusses the two-mode situation described by the linear coupling Hamiltonian (19), and relates it to the case of a 3MC with perfectly reflecting middle mirror of Ref. [6]. We consider specifically the situation where the frequencies of the two resonator modes under consideration are widely separated and are driven by two independent incident lasers of frequencies ω_{La} and ω_{Lb}, from the same side of the cavity. This implies an input mirror with transmissivity $T_{\rm end}$ and an end mirror with perfect reflectivity.

The quantum Langevin equations for the Hamiltonian of Eq. (19) can be written as

$$\dot{a} = -\left[i(\delta - \xi_L q) + \frac{\gamma}{2}\right]a + \sqrt{\gamma}a^{\rm in},$$

$$\dot{b} = -\left[i(\delta + \xi_L q) + \frac{\gamma}{2}\right]b + \sqrt{\gamma}b^{\rm in}, \quad \dot{q} = p/m,$$

$$\dot{p} = -m\omega_M^2 q + \hbar\xi_L(a^\dagger a - b^\dagger b) - \frac{D_M}{m}p + \epsilon^{\rm in}, \tag{B1}$$

where γ describes the decay rate of the 3MC, and the frequencies of the two lasers have been chosen such that

$$\delta = \omega_n - \delta_e - \omega_{La} = \omega_n + \delta_o - \omega_{Lb}. \tag{B2}$$

Equation (B1) is exactly the same as Eq. (3) of Ref. [6] with the change of notation $\xi \to \xi_L$, hence it yields the same radiation effects.

The effective parameters for the middle mirror can therefore be determined from Eq. (7) of Ref. [6], which we reproduce below

$$\omega_{\rm eff}^2 = \omega_M^2 - \frac{4\xi\gamma P_{\rm in}}{mL}\frac{\delta}{\delta^2 + \frac{\gamma^2}{4}}\frac{\left(\frac{\gamma}{2}\right)^2 - (\omega^2 - \delta^2)}{\left[\left(\frac{\gamma}{2}\right)^2 + (\omega - \delta)^2\right]\left[\left(\frac{\gamma}{2}\right)^2 + (\omega + \delta)^2\right]},$$

$$D_{\rm eff} = D_M + \frac{4\xi\gamma P_{\rm in}}{L}\frac{\delta}{\delta^2 + \frac{\gamma^2}{4}}\frac{\gamma}{\left[\left(\frac{\gamma}{2}\right)^2 + (\omega - \delta)^2\right]\left[\left(\frac{\gamma}{2}\right)^2 + (\omega + \delta)^2\right]}. \tag{B3}$$

Figure 5 shows that for an appropriate middle mirror position we can have $\xi_L \sim \xi$. Even for a mirror transmission as large as $T = 0.7$ [7], $\xi_L \sim \xi/2$ is possible, indicating that the cooling of the moving mirror to its ground state of vibration is possible both for weakly transparent as well as for perfectly reflecting mirrors using essentially the same parameters. It also follows that the advantages of the 3MC over the 2MC pointed out in Ref. [6] are retained even in the case where the middle mirror is partially transparent.

Table I lists the relevant numerical values considered in this paper. Using 5 mW of trapping light at a detuning $\delta_t = -2.5\gamma$ and 10 μW of cooling light at a detuning $\delta_c = 0.5\gamma$ we find $\omega_{\rm eff} \sim 300\omega_M$, $D_{\rm eff} \sim 10^6 D_M$, and $T_{\rm eff} \sim 200$ μK. Here we have assumed a mechanical quality factor of 10^6, an optical finesse of 10^5, and an ambient temperature of 300 K. From Eq. (2), these values imply $n_M < 1$. We note that in Eq. (3) of Ref. [6]. a and b are the annihilation operators of the modes in the subcavities, while in Eq. (B1) they correspond to modes of the full resonator; in the case of a finite transmission, both modes need to be pumped to ob-

tain a behavior analogous to that of the 3MC with the perfectly reflective middle mirrors. We finally remark that if we do not pump the odd mode [i.e., set $b \equiv 0$ in Eq. (19)], we obtain the 2MC Hamiltonian

$$H = \hbar(\omega_n - \delta_e)a^\dagger a + \frac{p^2}{2m} + \frac{1}{2}m\omega_M^2 Q^2 - \hbar\xi_L a^\dagger a Q, \quad \text{(B4)}$$

and hence can trap or cool with a single mode. In our proposal for a hybrid design for cooling and trapping in Sec. V, we red-detune from the even mode to achieve passive cooling.

APPENDIX C: STEADY STATE SOLUTIONS AND BISTABILITY

This appendix considers the bistability of the steady-state solutions in the case of a partially transparent mirror placed in such a way that the resonator frequency is at a minimum, see Eq. (33). The equations obtained by setting the time derivatives in Eq. (26) equal to zero are

$$b_s = \frac{\sqrt{\gamma}b_s^{\text{in}}}{i(\delta + \hbar\xi_Q q_s^2) + \frac{\gamma}{2}}, \quad p_s = 0, \quad 0 = -(\hbar\xi_Q|b_s|^2 + m\omega_M^2)q_s, \quad \text{(C1)}$$

where we have solved for p_s. The value of b_s can be obtained by using the first equation in the last and solving for q_s.

From the last equation we see that $q_s = 0$ is the only real solution for the mirror position. This is because the factor in parentheses is the sum of two positive nonzero terms, and can never equal zero for real q_s. Hence there is no bistability for the single-mode configuration of Sec. IV B.

[1] S. Gigan, H. R. Böhm, M. Paternostro, F. Blaser, G. Langer, J. B. Hertzberg, K. C. Schwab, D. Bäuerle, M. Aspelmeyer, and A. Zeilinger, Nature (London) **444**, 67 (2006).

[2] D. Kleckner and D. Bouwmeester, Nature (London) **444**, 75 (2006).

[3] O. Arcizet, P.-F. Cohadon, T. Briant, M. Pinard, and A. Heidmann, Nature (London) **444**, 71 (2006).

[4] A. Schliesser, P. Del'Haye, N. Nooshi, K. J. Vahala, and T. J. Kippenberg, Phys. Rev. Lett. **97**, 243905 (2006).

[5] T. Corbitt, Y. Chen, E. Innerhofer, H. Muller-Ebhardt, D. Ottaway, H. Rehbein, D. Sigg, S. Whitcomb, C. Wipf, and N. Mavalvala, Phys. Rev. Lett. **98**, 150802 (2007).

[6] M. Bhattacharya and P. Meystre, Phys. Rev. Lett. **99**, 073601 (2007).

[7] J. D. Thompson, B. M. Zwickl, A. M. Jayich, F. Marquardt, S. M. Girvin, and J. G. E. Harris, e-print arXiv:0707.1724v2.

[8] C. H. Metzger and K. Karrai, Nature (London) **432**, 1002 (2004).

[9] F. Marquardt, J. P. Chen, A. A. Clerk, and S. M. Girvin, Phys. Rev. Lett. **99**, 093902 (2007).

[10] A. Dorsel, J. D. McCullen, P. Meystre, E. Vignes, and H. Walther, Phys. Rev. Lett. **51**, 1550 (1983).

[11] Stabilization is usually implemented using electronic feedback, but all-optical stabilization has also been achieved [5]. From this perspective our proposal [6] for the 3MC offers an interesting way to control instabilities purely optically.

[12] We clarify that in passive cooling experiments—as opposed to cold damping experiments—the low-frequency part of the "error" signal is fed back to lock the cavity while the high frequency part is used to acquire the noise spectrum of the mirror. The force due to electronic feedback thus degrades quickly outside the low-frequency bandwidth ω_b which is much smaller than the effective response frequency of the mirror ω_{eff}. At ω_{eff} the radiation effects thus dominate the feedback force, leading to the mentioned asymmetric optical potential.

[13] P. Meystre, E. M. Wright, J. D. McCullen, and E. Vignes, J. Opt. Soc. Am. B **2**, 1830 (1985); J. D. McCullen, P. Meystre, and E. M. Wright, Opt. Lett. **9**, 193 (1984).

[14] F. Ya. Khalili, Phys. Lett. A **288**, 251 (2001).

[15] M. Vogel, C. Mooser, K. Karrai, and R. J. Warburton, Appl. Phys. Lett. **83**, 1337 (2003).

[16] B. S. Sheard, M. B. Gray, C. M. Mow-Lowry, D. E. McClelland, and S. E. Whitcomb, Phys. Rev. A **69**, 051801(R) (2004).

[17] B. M. Zwickl, W. E. Shanks, A. M. Jayich, C. Yang, A. C. Bleszynski Jayich, J. D. Thompson, and J. G. E. Harris, e-print arXiv:0711.2263v1.

[18] V. B. Braginsky, Y. I. Vorontsov, and K. S. Thorne, Science **209**, 547 (1980).

[19] I. Favero and K. Karrai, e-print arXiv:0707.3117.

[20] W. J. Fader, IEEE J. Quantum Electron. **21**, 1838 (1985).

[21] W. Weng Chow, IEEE J. Quantum Electron. **22**, 1174 (1986).

[22] S. Wieczorek and W. W. Chow, Phys. Rev. A **69**, 033811 (2004).

[23] We also note that the experimental arrangement corresponding to this model is that of the 3MC irradiated from both sides [6], unlike Fig. 1(b). In this case both end mirrors have a small transmissivity T_{end} (Table I).

[24] C. Gardiner, *Quantum Noise* (Springer-Verlag, Berlin, 1991).

[25] C. Genes, D. Vitali, P. Tombesi, S. Gigan, and M. Aspelmeyer, e-print arXiv:0705.1728v3; D. Vitali, P. Tombesi, M. J. Woolley, A. C. Doherty, and G. J. Milburn, Phys. Rev. A **76**, 042336 (2007); D. Vitali, S. Mancini, and P. Tombesi, J. Phys. A: Math. Theor. **40**, 8055 (2007); M. Paternostro, D. Vitali, S. Gigan, M. S. Kim, C. Brukner, J. Eisert, and M. Aspelmeyer, Phys. Rev. Lett. **99**, 250401 (2007).

[26] E. X. DeJesus and C. Kaufman, Phys. Rev. A **35**, 5288 (1987).

[27] P. F. Cohadon, A. Heidmann, and M. Pinard, Phys. Rev. Lett. **83**, 3174 (1999).

[28] S. Haroche, *Exploring the Quantum* (Oxford University Press, Oxford, 2006).

[29] E. K. Irish and K. Schwab, Phys. Rev. B **68**, 155311 (2003).

[30] M. LaHaye, J. Suh, P. Echtemach, K. Schwab, and M. Roukes, http://meetings.aps.org/link/BAPS.2007.MAR.A33.4